

Chiral tunneling through the single barrier structure based on the α -T3 model

A. M. Korol^{1,2}, A. I. Sokolenko², and O. Shevchenko²

¹Laboratory on Quantum Theory in Linköping, ISIR, P.O. Box 8017, S-580, Linköping, Sweden

²National University for Food Technologies, Kyiv, Ukraine

E-mail: korolam@ukr.net

Received March 30, 2020, revised December 14, 2020

published online February 26, 2021

The transmission coefficient T of the Dirac quasielectrons through a rectangular potential barrier in the α -T3 model is calculated and analyzed in the continuum approach. The dependence of the transmission rate on parameter α , which characterizes the degree of coupling of the central atom with the atoms in the vertices of the hexagonal lattice, and parameter β , which is equal to the ratio of Fermi velocities in the barrier and out-of-barrier regions, is analyzed. It was found, for certain quasiparticle energies, the supertunneling phenomenon is observed, which is that the transmission coefficient is equal to one independently of an angle of the particle incidence on the barrier, provided that $\alpha = 1$. The values of these energies depend on the barrier height and the parameter β . It is shown that for some sets of parameters the function $T(\alpha)$ has maxima in the range $0 < \alpha < 1$. For a large range of parameter values, the transmittance increases monotonically with increasing α . For the zero angle of incidence of quasiparticles on the barrier the Klein paradox is observed, i.e., the quantum transparency of the system is ideal, and this is true for any values of parameters α , β , barrier height, and energy of quasiparticles.

Keywords: α -T3 model, transmission coefficient, supertunneling.

Introduction

A lot of modern physical structures can be conveniently described using the so-called α -T3 model [1–8]. This model can rightly be attributed to a new class of objects that have received the name of the Dirac materials in recent years [9]. These include very different objects in their structure, in particular the low and high-temperature d -wave superconductors, superfluid phases of ^3He , graphene, two- and three-dimensional insulators, etc. [9]. The key concept that unites these different objects is a linear dispersion relation that describes the low-energy excitations of the quasiparticles. Due to the fact that the Dirac materials have a number of non-trivial, interesting properties, they are actively studied in the last time. Under low energies, the quasiparticle states of the Dirac materials are described by a massless Dirac equation in one or two dimensions, analogous to the equation for the quasielectrons in graphene. The dispersion relation for the Dirac particles relates to a cone in the three-dimensional case. Some properties of states in the Dirac materials are expressed in terms of topologically invariant quantities and, importantly, are protected from the influence of moderate perturbations due to the

symmetry of inversion of time in the corresponding Hamiltonian. Time reversal invariant perturbations such as lattice imperfections or non-magnetic moderate disorder do not produce a gap.

The α -T3 model is an intermediate structure between a dice lattice and graphene. It is characterized by the parameter α which determines the coupling strength between the central atom of the hexagonal lattice and the atoms in the hexagon vertices [1–8]. It is clear that different values of α correspond to different physical states of the α -T3 model and it was successfully applied to various physical structures [1–8].

At the same time, it is known that the characteristics of structures based on the Dirac materials are significantly influenced by the difference in the values of the Fermi velocity in different parts of the given structure [10–20]. A lot of various structures with non-equal Fermi velocities in different regions of the considered structure were studied in the last years. They include the graphene based single- and double-barrier structures, various types of superlattices including the quasiperiodic ones, superconducting junctions, structures based on the topological insulators, etc. [10–20].

Motivated by the above considerations, in this paper, we study the ballistic transmission of quasielectrons through a rectangular potential barrier in the α -T3 model and show that it depends strongly, in particular, on the relation between the parameters α and β . To be more exact, we consider the α -T3 model proposed in [1]. In this model, two sites per unit cell are associated with the hopping parameter t , and the connection between the additional site (placed at the center of each hexagon) with the site at the vertex of the hexagon is believed to be realized via the

hopping parameter αt . This model interpolates between two limiting cases: if $\alpha=0$ we deal with the pristine graphene, and if $\alpha=1$ the proposed model is reduced to the dice lattice. By changing the values of the parameters α and β , one can flexibly control the transmission properties of the structure under consideration within a wide range.

Model and Formulae

The Dirac-like equation for the considered model can be represented as follows [1–8]

$$\begin{pmatrix} 0 & \hbar v_F (k_x - ik_y) \cos \varphi & 0 \\ \hbar v_F (k_x + ik_y) \cos \varphi & 0 & \hbar v_F (k_x - ik_y) \sin \varphi \\ 0 & \hbar v_F (k_x + ik_y) \sin \varphi & 0 \end{pmatrix} \Psi + UI_0 \Psi = E \Psi, \quad (1)$$

where U is the external potential which corresponds to the rectangular barrier and is equal to: in the barrier region $U(0 < x < D) = U$ and $U = 0$ otherwise, I_0 is the identity matrix, k_x, k_y the quasimomentum components along $0x$ and $0y$ axis, the wave moves across the barrier ($0x$ axis).

For our purpose, it suffice to take into consideration only one K valley in the hexagonal Brillouin zone. The quantity v_F acquires different values in the barrier and out-of-barrier regions. The parameter φ is introduced for convenience, $\varphi = \arctan \alpha$, α is a parameter showing the coupling strength of the central atom with the atom at the hexagon vertice; for the dice lattice $\alpha=1$, for graphene $\alpha=0$.

The eigenfunctions in the Eq. (1) can be represented as follows

$$\Psi_I = \frac{1}{\sqrt{2}} \begin{pmatrix} \cos \varphi e^{i\phi} \\ 1 \\ \sin \varphi e^{-i\phi} \end{pmatrix} e^{ik_x x} e^{ik_y y} + \frac{r}{\sqrt{2}} \begin{pmatrix} -\cos \varphi e^{-i\phi} \\ 1 \\ -\sin \varphi e^{i\phi} \end{pmatrix} e^{-ik_x x} e^{ik_y y}, \quad (2)$$

$$\Psi_{II} = \frac{a}{\sqrt{2}} \begin{pmatrix} \cos \varphi e^{i\theta} \\ -1 \\ \sin \varphi e^{-i\theta} \end{pmatrix} e^{iq_x x} e^{ik_y y} - \frac{b}{\sqrt{2}} \begin{pmatrix} \cos \varphi e^{-i\theta} \\ 1 \\ \sin \varphi e^{i\theta} \end{pmatrix} e^{-iq_x x} e^{ik_y y}, \quad (3)$$

$$\Psi_{III} = \frac{t}{\sqrt{2}} \begin{pmatrix} \cos \varphi e^{i\phi} \\ 1 \\ \sin \varphi e^{-i\phi} \end{pmatrix} e^{ik_x x} e^{ik_y y}, \quad (4)$$

where index II refers to the barrier region and I, III refer to the out-of-barrier regions, ϕ, θ are the incidence and the refraction angle, respectively. Then the quasimomentums are equal to:

$$k_x = \sqrt{\frac{E^2}{(\hbar v_{F1})^2} - k_y^2}, \quad q_x = \sqrt{\frac{(E-U)^2}{(\hbar v_{F2})^2} - k_y^2},$$

$$\hbar v_{F1} k_x = E \cos \phi, \quad \hbar v_{F1} k_y = E \sin \phi, \quad \theta = \arctan(k_y / q_x). \quad (5)$$

Using the appropriate matching conditions at the interfaces [21, 22]:

$$\begin{aligned} & \sqrt{v_{F1}} [\cos \varphi \Psi_I(x=0^-) + \sin \varphi \Psi_{III}(x=0^-)] = \\ & = \sqrt{v_{F2}} [\cos \varphi \Psi_I(x=0^+) + \sin \varphi \Psi_{III}(x=0^+)], \\ & \sqrt{v_{F1}} \Psi_{II}(x=0^-) = \sqrt{v_{F2}} \Psi_{II}(x=0^+), \\ & \sqrt{v_{F2}} [\cos \varphi \Psi_I(x=D^-) + \sin \varphi \Psi_{III}(x=D^-)] = \\ & = \sqrt{v_{F1}} [\cos \varphi \Psi_I(x=D^+) + \sin \varphi \Psi_{III}(x=D^+)], \\ & \sqrt{v_{F2}} \Psi_{II}(x=D^-) = \sqrt{v_{F1}} \Psi_{II}(x=D^+) \end{aligned} \quad (6)$$

we can obtain the expression for the coefficient t :

$$t = 4 \cos \phi \cos \theta e^{-i(k_x + q_x)D} \{2[1 + \cos(\theta - \phi)] - 2[1 - \cos(\theta + \phi)] e^{-2i q_x D} - (1 - e^{-2i q_x D}) \sin^2(2\varphi) (\sin \theta + \sin \phi)^2\}^{-1}. \quad (7)$$

This formula is an agreement with the expression (18) from [11] in the case of $\alpha=0$ and with the expression (12) from [17] in the case of $\alpha=1$. The transmission coefficient T is equal to $T = |t|^2$.

Results and Discussion

Figures 1–3 show the transmission spectrum, i.e., the dependence of the transmission coefficient T on the quasielectron energy E (Fermi energy).

The spectra have a pronounced resonant-tunneling character. Two groups of different origin should be distinguished among the resonant peaks. First of all, let us distinguish the maxima corresponding to the energies $E_+ = 0.2$ eV and $E_- = 0.6$ eV in Fig. 1. These maxima refer to the phenomenon of the supertunneling, which means that the transparency of the given structure becomes perfect, i.e., the transmission coefficient becomes equal to one for all angles of incidence of quasielectrons on the barrier. We emphasize that this phenomenon occurs only for the value $\alpha=1$. As known [17], it is observed in structures based on the dice lattice, in which it is manifested for energy equal to half the height of the potential barrier: $E = U/2$. In the structure considered in this paper, the energies for which the supertunneling phenomenon is realized depend on the value of β . We can find this dependency from the formulae above and it reads:

$$E_{\pm} = \frac{U}{|1 \pm \beta|}. \quad (8)$$

Therefore, for each value of the potential barrier height U and the Fermi velocities in the barrier and out-of-barrier regions there are two energies for which the supertunneling is observed.

Another group of peaks with a maximum value of $T=1$ refers to the Fabry–Perot-type resonances resulting from the interference of electron waves. These resonances obey the formula

$$D \sqrt{\frac{(E-U)^2}{(\hbar v_2)^2} - k_y^2} = n\pi, \quad (9)$$

where $n = 1, 2, 3, \dots$

As can be seen from this formula, the Fabry–Perot resonances do not depend on the value of α , which is confirmed by Figs. 1, 2 on which we see that the Fabry–Perot peak positions on the energy axis are the same for all α values.

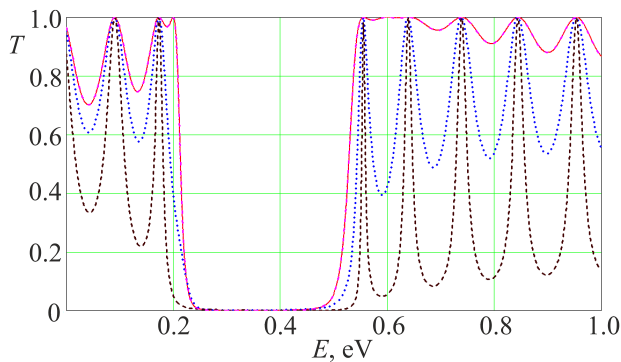


Fig. 1. (Color online) The dependence of the transmission coefficient T on the quasielectron energy E . The parameter values are as follows: $U = 0.3$ eV, $\phi = 1$ rad, $\beta = 0.5$, $D = 10$ nm; dashed (brown), dotted (blue), and solid (magenta) lines correspond to the values of $\alpha = 0.3, 0.7$, and 1 , respectively.

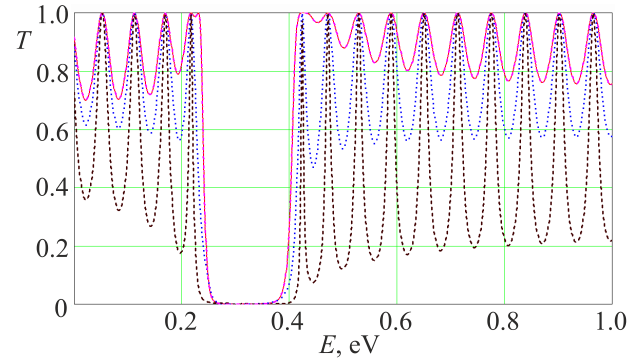


Fig. 2. (Color online) T vs E dependence for the parameter values: $U = 0.3$ eV, $\phi = 1$ rad, $\beta = 0.3$, $D = 10$ nm; dashed (brown), dotted (blue), and solid (magenta) lines correspond to the values of $\alpha = 0.3, 0.7$, and 1 , respectively.

At the same time, the values of the transmission coefficient T for the energies located between the resonant peaks depend significantly on α , and they increase markedly with increasing in α .

A marked characteristic of these spectra is the presence in them of the energy gap — the band in which the value of T is close to zero. This band is located around the energies close to the top of the potential barrier $E \sim U$, and its origin is due to the fact that, for these energies, the quasi-momentum in the barrier region becomes imaginary [see Eq. (5)] and the electron wave decays [see Eqs. (2)–(4)].

The spectra $T(E)$ are very sensitive to the values of the parameter β . Thus, with increasing β , the energy gap increases significantly; the number of the Fabry–Perot resonances in the fixed energy range markedly decreases (Figs. 1–3).

The analyzed spectra also have a pronounced angular dependence, that is, the values of the transparency coefficient T strongly depend on the angle of incidence of the quasiparticles on the potential barrier. We will dwell more on this dependence below, and here we will pay attention

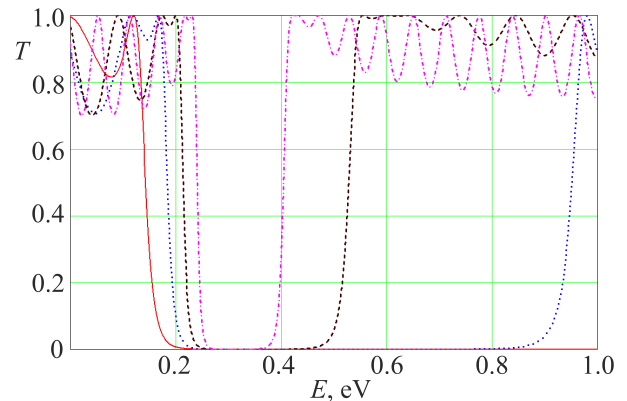


Fig. 3. (Color online) T vs E dependence for the parameter values: $U = 0.3$ eV, $\phi = 1$ rad, $\alpha = 1$, $D = 10$ nm; dashed and dotted (magenta), dashed (brown), dotted (blue), and solid (red) lines correspond to the values of $\beta = 0.3, 0.5, 0.8$, and 1.5 , respectively.

to the presence of the so-called critical angle of incidence ϕ_c — such that for all incidence angles $\phi > \phi_c$ the barrier becomes completely opaque. The value of the critical angle of incidence can be found from the Snell's law, and it is equal to:

$$\phi_c = \pm \arcsin\left(\frac{|E-U|}{\beta E}\right). \quad (10)$$

In particular, for the parameters for Fig. 3 the largest value of β leads to that the angle $\phi = 1$ rad is already greater than the critical one: see the corresponding solid (red) line. The other curves in this figure correspond to the angles less than the critical one (here $\alpha=1$ for all curves). We would like to note that according to Eq. (10) the critical angle depends on both quantities U and E , it can be observed for $\beta > 1$ as well as for $\beta < 1$. In case of absence of the electrostatic potential ($U = 0$) the critical angle can be realized only for values of $\beta > 1$ (see, e.g., [14, 15]).

Note that the lines $T(E)$ for different values of α are the curves with inflection. This inflection becomes more pronounced with increasing α until the coefficient T reaches its maximum value $T = 1$, which corresponds to the phenomenon of the supertunneling at $\alpha=1$ (see the gradual transformation of the lines $T(E)$ with change in α in Fig. 4). Note that these inflexions affect the dependence on energy of the conductivity and of the Fano factor of the considered structure.

In order to analyze in more details the dependence of the transparency coefficient T on the parameter α , it is convenient to use the image of the function $T(\alpha)$ presented in Fig. 5.

The obtained spectra are very sensitive to the changes in the parameter values. For most of them, there is a tendency: the magnitude of T increases with increase in α . At the same time the most striking feature of the function $T(\alpha)$ is its non-monotonicity, namely the presence of a maximum for a certain value of α (in the range $0 < \alpha < 1$). So we have an important conclusion: in a certain range of

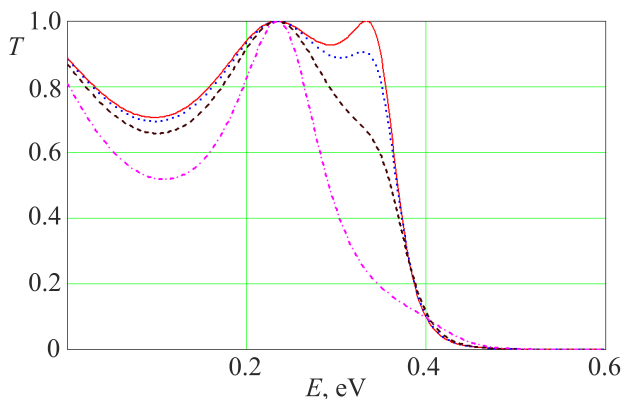


Fig. 4. (Color online) T vs E dependence for the parameter values: $U = 0.3$ eV, $\phi = 1$ rad, $D = 10$ nm, $\beta = 0.8$; solid (red); dotted (blue), dashed (brown), dashed and dotted (magenta) lines correspond to the values of $\alpha = 1, 0.9, 0.8$, and 0.6 , respectively.

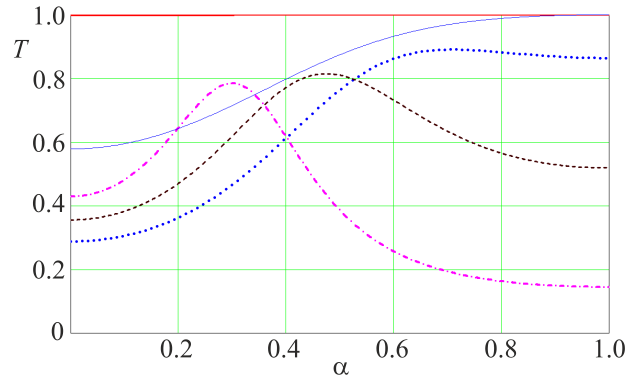


Fig. 5. (Color online) T vs α dependence for the parameter values: for all lines $D = 2$ nm, $\phi = 1$ rad; for the thick solid (red), and thin solid (blue) lines $E = 0.2$ eV, $U = 0.3$ eV, for other curves $E = 0.02$ eV, $U = 0.03$ eV; thick solid (red), thin solid (blue), dotted (blue), dashed (brown), dashed and dotted (magenta) lines correspond to the values of $\beta = 0.156, 0.5, 0.8, 1.35$, and 3 , respectively.

the parameter values (quite a narrow one) the transmission reaches a maximum value and this maximum is realized for some intermediate values of α (between 0 and 1, not for $\alpha=1$). This conclusion is echoed by a series of works [1–8] showing that some physical properties will prove to reveal the non-monotonic dependence on α . For example, in [7] it is shown that the Hall conduction has the additional steps only for certain intermediate (between 0 and 1) values of α . In connection with the above, one can note the works of [2, 4, 5], which investigated the magneto-optical conductivity, orbital magnetic susceptibility and the Hofstadter butterfly. They also emphasized the importance of intermediate values of α .

It is known that in graphene or graphene structures, a special selection of parameter values can lead to special effects or results. The same situation is relevant to the structure considered in this work. In particular, for the values of the parameters $E = 0.2$ eV, $U = 0.4$ eV, $D = 10$ nm, $\beta \approx 0.7$, the transmission coefficient T is almost equal to one in the whole range of incidence angle, provided that $\alpha=1$, see Fig. 6. For other values of α , the value of T is also high. In fact, here we have a result close to the supertunneling.

The dependence of $T(\phi)$ displays the unordinary behavior for the value $\beta \approx 0.7$ comparing with other β values (see Fig. 7): there is a decrease in T with increasing of ϕ starting from zero, but after reaching a value $\phi \approx 0.37\pi$ the coefficient T begins to increase until the certain angle near $\phi = \pi/2$ is reached, after which the value of T drops sharply to zero. Note that for this set of the parameter values, the magnitude of T is high even for small α .

Note that the transmission of the quasielectrons through a given structure depends essentially on the values of the parameter α , as well as on the values of the parameter β , that is, substantially depends on the interplay between α and β .

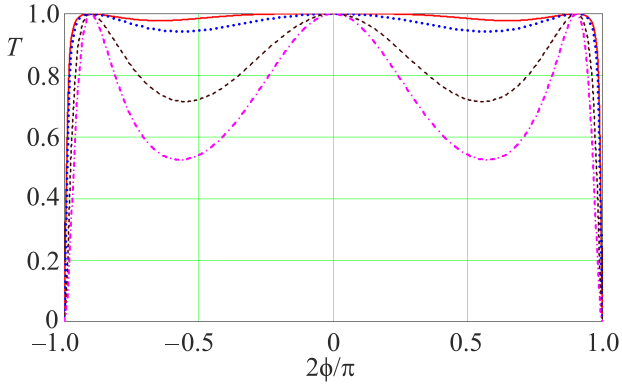


Fig. 6. (Color online) T vs ϕ dependence for the values of the parameters: for all lines $E = 0.2$ eV, $U = 0.4$ eV, $D = 10$ nm, $\beta \approx 0.7$; solid (red), dotted (blue), dashed (brown), and dashed-dotted (magenta) lines correspond to the values of $\alpha = 1, 0.8, 0.5,$ and $0.3,$ respectively.

For most values of the parameters of this problem, the region of the incidence angles with a high value of T is wider for larger α and smaller β , and the values of the coefficient T for a fixed angle increase with increasing of α and decreasing in β .

Figures 6, 7 show that in the structure considered there is an effect similar to the Klein paradox: for the normal incidence of quasiparticles on the barrier, it becomes perfectly transparent, that is, the value of the coefficient T is equal to unity, regardless of the value of the barrier height U and its thickness D . We emphasize that in this case $T = 1$ also independently on the values of the parameters α and β .

Figure 8 illustrates the dependence of T on α for different incidence angles.

Let us dwell further on the dependence of T on the thickness of the potential barrier D . In this dependence we ob-

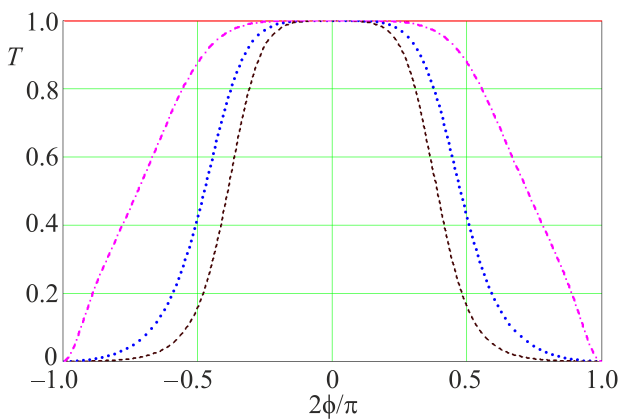


Fig. 7. (Color online) T vs ϕ dependence for the values of the parameters $E = 0.2$ eV, $U = 0.3$ eV, $D = 10$ nm, $\beta = 0.5$; solid (red), dashed-dotted (magenta), dotted (blue), and dashed (brown) lines correspond to the values of $\alpha = 1, 0.8, 0.5,$ and $0.1,$ respectively.

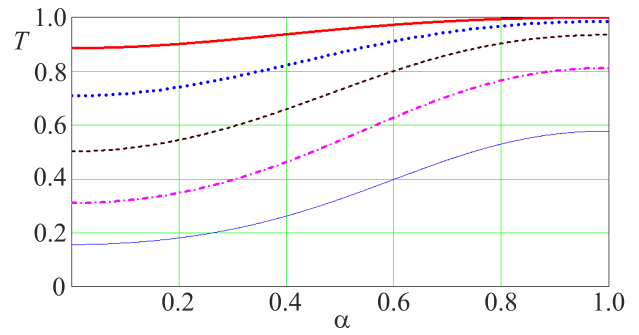


Fig. 8. (Color online) T vs α dependence for different incident angles, the parameters are as follows: for all lines $E = 0.2$ eV, $U = 0.6$ eV, $D = 10$ nm, $\beta = 0.35$; thick solid (red), dotted (blue), dashed (brown), dashed and dotted (magenta), and thin solid (blue) lines correspond to the values of $\phi = 0.3, 0.5, 0.7, 0.9,$ and 1.1 rad, respectively.

serve several different modes. They are presented in Fig. 9. The dashed line corresponds to the phenomenon of the supertunneling, which is independent of the magnitude of D . The value of $\beta = 0.3$ (for other fixed parameters) corresponds to the oscillating function with D — the dotted line in Fig. 9. Note that the horizontal line with $T = 1$ in Fig. 4 of [14, 15] refers to the Klein-like tunneling whereas the dashed line in Fig. 9 is related to the supertunneling. Finally, the descending curves $T(D)$ ($\beta = 0.6$ and 0.7) correspond to such set of the parameters for which the existing barrier leads to a monotonous decrease in the magnitude of the transparency coefficient as the thickness of the barrier increases — as in the case of the conventional tunneling. As the thickness of the barrier increases, the number of resonances of the Fabry–Perot type increases and this number, like the position of the peaks on the 0ϕ axis, does not

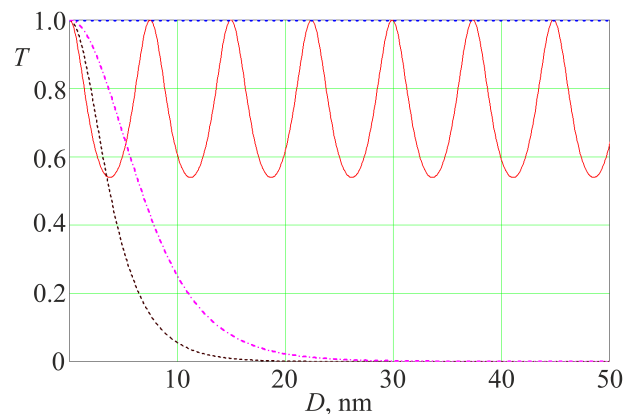


Fig. 9. (Color online) Dependence of the transmission coefficient T on the barrier thickness D for the parameters: $E = 0.2$ eV, $U = 0.3$ eV, $\phi = 1.2$ rad, $\alpha = 1$; solid (red), dotted (blue), dashed-dotted (magenta), and dashed (brown) lines correspond to the values of $\beta = 0.3, 0.5, 0.6,$ and $0.7,$ respectively.

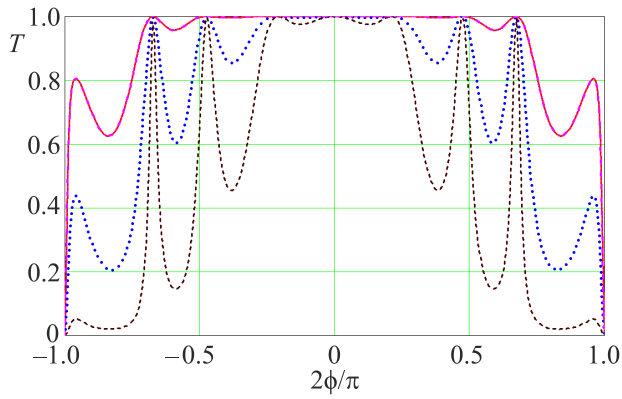


Fig. 10. (Color online) T vs ϕ dependence for the values of the parameters $E = 0.25$ eV, $U = 0.4$ eV, $D = 50$ nm, $\beta = 0.5$; solid (magenta), dotted (blue), and dashed (brown) lines correspond to the values of $\alpha = 1, 0.7$, and 0.3 , respectively.

depend on α ; but the value of T for the angles placed between the Fabry–Pérot resonances depends on α , increasing with increasing α . These affirmations are evidenced by Fig. 10 for value of $D = 50$ nm.

Figure 11 shows the dependence of $T(E)$ for the barrier thickness larger than in Fig. 1, namely $D = 20$ nm. Here, such changes in the graph $T(E)$ are observed: the oscillation frequency increases and half the width of the resonant peaks decreases with D . The energy gap becomes more pronouncedly formed.

Conclusions

Transmission properties of the single-barrier structure based on the α -T3 model are considered in the paper. It is believed that the barrier is sharp and has a rectangular shape. The physical origin of the barrier is assumed to be electrostatic, but it is taken into account that the Fermi velocities in the barrier and out-of-barrier regions have different values and this situation is referred to in the literature as the presence of the Fermi velocity barrier. The parameter α in this model can acquire values from zero to

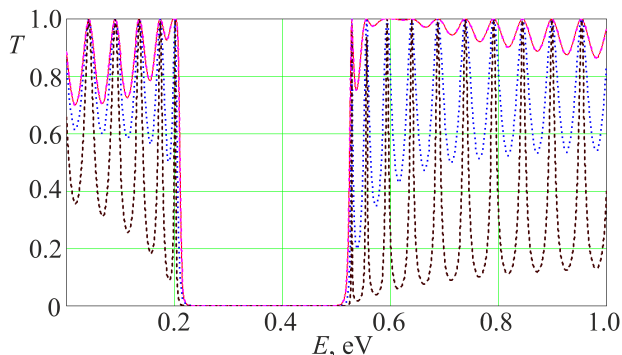


Fig. 11. (Color online) T vs E dependence for the values of the parameters $U = 0.3$ eV, $\phi = 1$ rad, $\beta = 0.5$, $D = 20$ nm; the dashed (brown), dotted (blue), and solid (magenta) lines correspond to the values of $\alpha = 0.3, 0.7$, and 1 , respectively.

one, moreover the case $\alpha = 0$ corresponds to graphene and $\alpha = 1$ to the dice lattice. Particular attention is given in the work to intermediate values of α , since, as is known from the literature, they are important for observing for a lot of physical phenomena. The transmission coefficient is found by means of matching of wave functions at the interfaces. The obtained spectra show a pronounced dependence on an angle of incidence of the pseudo-relativistic Dirac quasiparticles on the barrier of the structure under consideration. In particular, for the normal incidence angle there is a perfect penetration of particles through the barrier for any values of the parameters α , β , as well as of the barrier height and thickness, that is, an effect similar to the Klein paradox is realized here. At the same time for certain quasiparticle energies we observe the effect of the super-tunneling, which is that for these energies the barrier of the system becomes absolutely quantum-transparent for any angle of incidence of the particles on the barrier. Formula for these energies depending on the problem parameters is presented. For a given set of the parameter values, there are two energy values of quasielectrons, for which this phenomenon is realized. This unconventional feature can be useful for designing “a perfect focusing lens without loss” [17]. Also we show that for some special parameter sets there is a phenomenon similar to the supertunneling, i.e., the transmission rates is almost equal to unity for all incident angles. The spectra reveal the presence of the non-monotonicity in the $T(\alpha)$ dependence, namely there is maximum of the $T(\alpha)$ function. This circumstance is associated with the fact that some physical phenomena are observed for an intermediate (between zero and unity) values of α . The dependence of the transmission spectra on the barrier thickness is non-trivial, and qualitatively different modes of this dependence are possible. The spectra are sensitive to the interplay between α and β values, and they also substantially depend on other of the problem parameters. The obtained results may be useful in the modern nanoelectronics based on the Dirac materials.

1. A. Raoux, M. Morigi, J.-N. Fuchs, F. Piéchon, and G. Montambaux, *Phys. Rev. Lett.* **112**, 026402 (2014).
2. F. Piéchon, J.-N. Fuchs, A. Raoux, and G. Montambaux, *J. Phys.: Conf. Ser.* **603**, 012001 (2015).
3. J. D. Malcolm and E. J. Nicol, *Phys. Rev. B* **92**, 035118 (2015).
4. E. Illes and E. J. Nicol, *Phys. Rev. B* **94**, 125435 (2016).
5. Á. D. Kovács, G. Dávid, B. Dóra, and J. Cserti, *Phys. Rev. B* **95**, 035414 (2017).
6. T. Biswas and T. K. Ghosh, *J. Phys.: Condens. Matter* **28**, 495302 (2016).
7. E. Illes, J. P. Carbotte, and E. J. Nicol, *Phys. Rev. B* **92**, 245410 (2015).
8. E. Illes and E. J. Nicol, *Phys. Rev. B* **95**, 235432 (2017).
9. T. O. Wehling, A. M. Black-Schaffer, and A. V. Balatsky, *Adv. Phys.* **63**, 1 (2014).

10. Lei Liu, Yuxian Li, and Jian-Jun Liu, *Phys. Lett. A* **376** No. 45, 3342 (2012).
11. Y. Wang, Y. Liu, and B. Wang, *Physica E* **53**, 186 (2013).
12. Li-Feng Sun, Chao Fang, and Tong-Xiang Liang, *Chin. Phys. Lett.* **30**, 047201 (2013).
13. A. Raoux, M. Polini, R. Asgari, A. R. Hamilton, R. Fasio, and A. H. MacDonald, *Phys. Rev. B* **81**, 073407 (2010).
14. A. Concha and Z. Tešanović, *Phys. Rev. B* **82**, 033413 (2010).
15. J. H. Yuan, J. J. Zhang, Q. J. Zeng, J. P. Zhang, and Z. Cheng, *Physica B* **406**, 4214 (2011).
16. P. M. Krstajic and P. Vasilopoulos, *J. Phys. Condens. Matter* **23**, 135302 (2011).
17. Daniel F. Urban, Dario Bercioux, Michael Wimmer, and Wolfgang Hausler, *Phys. Rev. B* **84**, 115136 (2011).
18. A. M. Korol, N. V. Medvid, and A. I. Sokolenko, *Phys. Status Solidi* **255**, 1800046 (2018).
19. A. M. Korol and N. V. Medvid, *Fiz. Nizk. Temp.* **45**, 1311 (2019) [*Low Temp. Phys.* **45**, 1117 (2019)].
20. A. M. Korol, *Fiz. Nizk. Temp.* **45**, 576 (2019) [*Low Temp. Phys.* **45**, 493 (2019)].
21. R. Takahashi and S. Murakami, *Phys. Rev. Lett.* **107**, 166805 (2011).
22. Diptiman Sen and Oindrila Deb, *Phys. Rev. B* **85**, 245402 (2012).

Кіральне тунелювання через однобар'єрну структуру на основі моделі α -ТЗ

A. M. Korol, A. I. Sokolenko, O. Shevchenko

У рамках континуального підходу обчислено та проаналізовано коефіцієнт пропускання T квазіелектронів Дірака крізь прямокутний потенціальний бар'єр у моделі α -ТЗ. Проаналізовано залежність коефіцієнта пропускання від параметра α , який характеризує ступінь зв'язку центрального атома з атомами у вершинах гексагональної ґратки, та параметра β , який дорівнює відношенню швидкостей Фермі в бар'єрній та позабар'єрній областях. Встановлено, що для певних енергій квазічастинок спостерігається феномен супертунелювання, тобто коефіцієнт пропускання дорівнює одиниці незалежно від кута падіння частинок на бар'єр, за умови, що $\alpha = 1$. Значення цих енергій залежать від висоти бар'єру та величини параметра β . Показано, що для деяких наборів значень параметрів функція $T(\alpha)$ має максимуми в інтервалі $0 < \alpha < 1$. Для значного діапазону значень параметрів коефіцієнт пропускання монотонно зростає зі збільшенням α . Для нульового кута падіння квазічастинок на бар'єр спостерігається парадокс Клейна, тобто квантова прозорість системи є ідеальною, і це справедливо для будь-яких значень параметрів α , β , висоти бар'єру та енергії квазічастинок.

Ключові слова: α -ТЗ модель, коефіцієнт трансмісії, супертунелювання.